Design of Two-Dimensional Recursive Filters by Interpolation

HYOKANG CHANG AND J. K. AGGARWAL, FELLOW, IEEE

Abstract—**A technique for rotating the frequency responses of separable filters is developed. In this technique transfer functions having rational powers of z are introduced and realized by input/output signal array interpolations. Several applications of this technique to designing two-dimensional recursive filters are presented. Two- and multi-dimensional manipulations are performed by a series of one-dimensional manipulations.**

I. Introduction

RECURSIVE digital filtering of two- and multi-dimensional signals is an important technique in the processing of two- and multi-dimensional data. However, the design of two- and multi-dimensional recursive filters is difficult due to the fact that polynomials in two or more variables may not, in general, be factored into lower order polynomials. This difficulty can be partly circumvented by designing two- and multi-dimensional systems as one-dimensional systems. Shanks, Treitel, and Justice [1] proposed two methods for synthesizing two-dimensional recursive filters, one in the spatial domain and the other in the frequency domain. Manry and Aggarwal [2] have developed an implementation of a two-dimensional recursive filter as a one-dimensional recursive filter. Mersereau and Dudgeon [3] have presented a similar technique to that of [2] where two-dimensional sequences are represented as one-dimensional sequences. An alternative approach utilizing separable planar filters has been suggested by Treitel and Shanks [4].

The present paper develops a technique for rotating the frequency responses of separable filters. The resulting filters are separable with respect to the rotated frequency axes whereas Shanks' rotated filters are not. The transfer function of a separable filter is essentially a product of one-dimensional functions. In the present technique, transfer functions having rational powers of z are introduced and realized by input/output signal array interpolations.

Several applications of the technique to designing two-dimensional recursive filters are presented. A circularly symmetric low pass filter, a nonseparable bandpass filter, and a ring-shaped bandpass filter are designed to illustrate the procedure.

Manuscript received September 26, 1975; revised January 7, 1977. This work was supported in part by the Joint Services Electronics Program under JSEP Contract F44620-70-C-0091, and in part by NFS Grant GK 42790.

The authors are with the Department of Electrical Engineering, University of Texas at Austin, Austin, TX 78712.

II. Preliminaries

A. Difference Equations for Digital Filters

A one-dimensional recursive digital filter is described by the linear difference equation

$$g_n = \sum_{k=0}^{u} b_k f_{n-k} - \sum_{k=1}^{v} c_k g_{n-k} \tag{1}$$

and the corresponding transfer function is

$$H(z) = \frac{G(z)}{F(z)} = \frac{b_0 + b_1 z + \cdots + b_u z^u}{1 + c_1 z + \cdots + c_v z^v} \tag{2}$$

where u and v are nonnegative integers. Similarly a two-dimensional recursive filter is described by the spatial difference equation

$$g(M,N) = \sum_{m=0}^{r} \sum_{n=0}^{s} b(m,n) f(M-m, N-n) - \sum_{\substack{m=0 \\ (m,n)\neq(0,0)}}^{p} \sum_{n=0}^{q} c(m,n)\, g(M-m, N-n) \tag{3}$$

and the corresponding transfer function is

$$H(z_1,z_2) = \frac{G(z_1,z_2)}{F(z_1,z_2)} = \frac{\sum_{m=0}^{r} \sum_{n=0}^{s} b(m,n) z_1^m z_2^n}{\sum_{m=0}^{p} \sum_{n=0}^{q} c(m,n) z_1^m z_2^n} \tag{4}$$

with $c(0,0)=1$. G and g denote output signals while F and f denote input signals. The numbers r, s, p, and q are nonnegative integers. It is assumed that $f(m,n)=0$ for m or n negative and that $g(m,n)$ is an initial condition for m or n negative.

B. Causality, Stability, and Finite Area Array

Causality: A two-dimensional filter is said to be realizable or causal if its impulse response satisfies the property [5], [6]

$$h(m,n)=0, \qquad \text{for } m<0 \text{ or } n<0. \tag{5}$$

Stability: A two-dimensional filter is said to be stable if and only if its impulse response satisfies the con-

straint [5], [6]

$$\sum_{m=-\infty}^{+\infty}\sum_{n=-\infty}^{+\infty}|h(m,n)|<\infty. \tag{6}$$

Finite Area Array: A two-dimensional array that is nonzero for only a finite area in the spatial domain is referred to as a finite area array [5].

For a finite area array $A(M_1\times N_1)$, simple array reorientations are possible which include:

1) 90° rotation

$$\hat{A}(m,n)=A(n,N_1-m+1)$$

2) transposition

$$\hat{A}(m,n)=A(n,m)$$

3) 180° rotation about $M_1/2$-axis (mirror image)

$$\hat{A}(m,n)=A(M_1-m+1,n)$$

4) 180° rotation about $N_1/2$-axis (mirror image)

$$\hat{A}(m,n)=A(m,N_1-n+1)$$

where $A(m,n)$ and $\hat{A}(m,n)$ denote the original and reoriented arrays, respectively.

C. Sampling Theorem and Interpolation Functions

For a one-dimensional function $f(t)$ the sampling theorem is stated as follows [7].

If the Fourier transform of a function $f(t)$ is zero above a certain frequency ω_c

$$F(\omega)=0, \qquad \text{for } |\omega|>\omega_c$$

then $f(t)$ can be uniquely determined from its values

$$f_n=f(nT)$$

at a sequence of equidistant points, a distance T apart. In fact $f(t)$ is given by

$$f(t)=\sum_{n=-\infty}^{+\infty} f_n \operatorname{sinc}\left(\frac{t}{T}-n\right) \tag{7}$$

where $T=\pi/\omega_c$ and $\operatorname{sinc}(x)=\sin(\pi x)/\pi x$.

Furthermore, given an arbitrary function $f(t)$ and a constant T, consider the function

$$d(t)=\sum_{n=-\infty}^{+\infty} f(nT)\operatorname{sinc}\left(\frac{t}{T}-n\right). \tag{8}$$

Now $d(nT)=f(nT)$ and the spectrum of $d(t)$ equals zero for $|\omega|>\omega_c$. Thus $d(t)$ offers a band-limited interpolation of $f(t)$. Likewise for an arbitrary two-dimensional function $f(x,y)$, the band-limited interpolation $d(x,y)$ is given by [8] as

$$d(x,y)=\sum_{m=-\infty}^{+\infty}\sum_{n=-\infty}^{+\infty} f(mL_x,nL_y)\operatorname{sinc}\left(\frac{x}{L_x}-m\right)\operatorname{sinc}\left(\frac{y}{L_y}-n\right) \tag{9}$$

where L_x and L_y are sample intervals and $d(mL_x,nL_y)=f(mL_x,nL_y)$. Further, $d(x,y)=f(x,y)$ if

$$F(\omega_x,\omega_y)=0, \qquad \text{for } |\omega_x|>\omega_{x_c} \text{ or } |\omega_y|>\omega_{y_c}$$

where $\omega_{x_c}=\pi/L_x$ and $\omega_{y_c}=\pi/L_y$.

Thus interpolation is accomplished by injecting at each sample point an interpolation function consisting of a product of sinc functions. This is by no means the only possible interpolation function. In general, $d(x,y)$ can be thought of as an expansion of the continuous spatial signal in the form [5]

$$d(x,y)=\sum_{m=-\infty}^{+\infty}\sum_{n=-\infty}^{+\infty} f_{mn}\varphi_{mn}(x,y) \tag{10}$$

where $\varphi_{mn}(x,y)$ is an interpolation function. There are several classes of interpolation functions that can be used to express a continuous spatial function in the form of (10), including sinusoidal functions, Laguerre functions, and Legendre polynomials.

D. Shanks' Rotated Filters

Given a two-dimensional filter that varies in one dimension only as

$$H_2(s_1,s_2)=H_1(s_1) \tag{11}$$

a rotated filter may be obtained by rotating the axes of the (s_1,s_2)-plane by an angle $-\theta$ [1]. Let (s_1,s_2) and $(\hat{s}_1,\hat{s}_2)$ represent original and rotated axes, respectively. Then,

$$\begin{bmatrix} s_1 \\ s_2 \end{bmatrix}=\begin{bmatrix} \cos\theta & \sin\theta \\ -\sin\theta & \cos\theta \end{bmatrix}\begin{bmatrix} \hat{s}_1 \\ \hat{s}_2 \end{bmatrix}. \tag{12}$$

Substituting (12) into (11), one gets

$$\hat{H}_2(\hat{s}_1,\hat{s}_2)=H_1(\cos\theta\cdot\hat{s}_1+\sin\theta\cdot\hat{s}_2). \tag{13}$$

This filter varies in both frequency directions. To produce the equivalent two-dimensional discrete filter, one uses the bilinear z-transform

$$\hat{s}_1=\frac{2}{L_1}\frac{1-z_1}{1+z_1}$$

$$\hat{s}_2=\frac{2}{L_2}\frac{1-z_2}{1+z_2}$$

where L_1 and L_2 are sample intervals. The overall transformation becomes

$$s_1=\cos\theta\left(\frac{2}{L_1}\right)\frac{1-z_1}{1+z_1}+\sin\theta\left(\frac{2}{L_2}\right)\frac{1-z_2}{1+z_2}$$

$$s_2=-\sin\theta\left(\frac{2}{L_1}\right)\frac{1-z_1}{1+z_1}+\cos\theta\left(\frac{2}{L_2}\right)\frac{1-z_2}{1+z_2}. \tag{14}$$

By substituting (14) into (11), one can get a two-dimensional digital filter

$$H(z_1,z_2)=H_1(s_1)|_{s_1=s_1(z_1,z_2)} \tag{15}$$

where the frequency response $H(e^{-j\omega_1 L_1},e^{-j\omega_2 L_2})$ has been rotated by an angle θ with respect to that of the reference filter, $H_0(z_1,z_2)$, obtained by setting $\theta=0$. However, the frequency response is no longer an exact rotated version of the reference filter response and tends to be distorted at higher spatial frequencies. This effect is caused by the bilinear transform.

III. Rotated Filters in the (z_1,z_2)-Plane

The frequency transformation technique is one of the traditional approaches in deriving desired frequency selective filters from simple prototype filters. This technique has been applied to one-dimensional digital filters [5], [6], and its extension to two-dimensional digital filters has been proposed by Pendergrass *et al.* [9]. Extending the notion of frequency transformation to include rational powers of z_1 and z_2, one can rotate the frequency response with band contraction. To begin with, consider the problem of rotating the frequency response which is related to the material of Section II-D.

For a causal and stable two-dimensional filter, described as in (11) by

$$H_2(z_1,z_2)=H_1(z_1) \tag{16}$$

consider the transformation

$$z_1=\hat{z}_1\hat{z}_2^{\beta/\alpha} \tag{17}$$

where α and β are integers. The corresponding frequency transformation is

$$\exp(-j\omega_1 L_1)=\exp(-j\hat{\omega}_1\hat{L}_1)\exp\left(-j\frac{\beta}{\alpha}\hat{\omega}_2\hat{L}_2\right)$$

$$=\exp\left[-j\left(\hat{\omega}_1\hat{L}_1+\frac{\beta}{\alpha}\hat{\omega}_2\hat{L}_2\right)\right]$$

or

$$\omega_1 L_1=\hat{\omega}_1\hat{L}_1+\frac{\beta}{\alpha}\hat{\omega}_2\hat{L}_2 \tag{18}$$

where $L_1^2=\hat{L}_1^2+(\beta/\alpha\hat{L}_2)^2$ and the angle of rotation is

$$\theta=\arctan\left(\frac{\beta}{\alpha}\right). \tag{19}$$

The responses before and after the transformation with $\beta/\alpha=1/2$ are shown in Fig. 1 where (16) represents a low-pass filter. In this figure, $\hat{L}_1$ and $\hat{L}_2$ are assumed to be unity. Note that $(\omega_{1c},0)$ and $(-\omega_{1c},0)$ are fixed points under the mapping of (18).

Now the transformation of (17) and its effects on the resulting filter $H_1(\hat{z}_1\hat{z}_2^{\beta/\alpha})$ may be examined in detail.

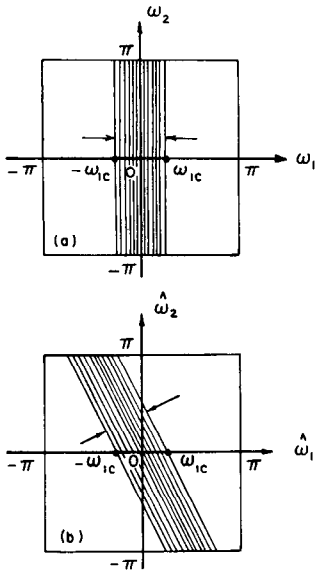

Fig. 1. Frequency response of low-pass filter of (16) and its rotated version ($\beta/\alpha=\frac{1}{2}$).

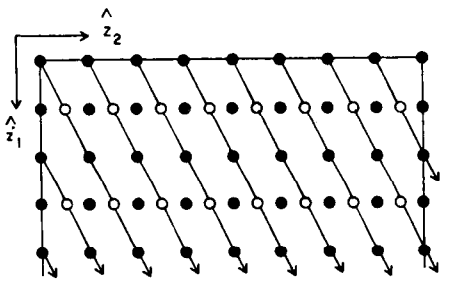

Fig. 2. Recursion directions of transformed filter ($\beta/\alpha=\frac{1}{2}$).

1) It may be thought of as a mapping from the unit circles of the $(\hat{z}_1,\hat{z}_2)$-plane into the unit circles of the (z_1,z_2)-plane.

2) When $\beta/\alpha\geq 0$, the transformation is causal, otherwise it is noncausal [see (5)].

3) In the spatial domain it is equivalent to the rotation of recursion direction with a new sample interval. The transformed recursing scheme of the filter in (16) with $\beta/\alpha=1/2$ is shown in Fig. 2.

4) In the frequency domain the effect of the transformation is a rotation of the frequency response with a contraction of the bandwidth as seen in Fig. 1. Since the filter of (16) is one-dimensional, we can extend the concept of bandwidth in one dimension to two dimensions along the frequency response varying direction. The bandwidth of the passband is contracted by the ratio of $\cos\theta$ ($\theta=\arctan(\beta/\alpha)$).

5) It is clear that the stability of the resulting filter is not affected since the transformation can be viewed as a transformation of the delay unit which may be specified by both recursing direction and sampling interval. (Assume that the input data is available at any spatial point.)

In observation 2) above, the transformation with $\beta/\alpha < 0$ may be utilized when noncausal recursions are available. For a finite area array input, one can always choose a causal recursion direction by reorienting the input signal array according to the ways listed in Section II-B. Referring to observation 3) and Fig. 2, it is clear that an input signal array must be defined at the new grid points so that the transformation of (17) may be meaningful. The discussion of this is deferred to the next section. As seen in observation 4), the transformation of (17) makes it possible to rotate the frequency response. The transformed filter $H_1(\hat{z}_1\hat{z}_2^{\beta/\alpha})$, which is obtained by substitution of (17) into (16), will be referred to as a (z_1,z_2)-plane rotated filter. To avoid confusion, Shanks' rotated filter will be referred to as an (s_1,s_2)-plane rotated filter. Observations 3) and 5) may be further clarified by examining the impulse responses of the original and transformed filters. In terms of the impulse response, the filter in (16) may alternately be described as

$$H_2(z_1,z_2)=\sum_{m=0}^{+\infty}\sum_{n=0}^{+\infty}h(m,n)z_1^m z_2^n$$

$$=\sum_{m=0}^{+\infty}h(m,0)z_1^m \tag{20}$$

where

$$h(m,n)=0, \qquad \text{for } m<0 \text{ or } n\neq 0. \tag{21}$$

Also,

$$\sum_{m=-\infty}^{+\infty}\sum_{n=-\infty}^{+\infty}|h(m,n)|=\sum_{m=0}^{+\infty}|h(m,0)|<\infty \tag{22}$$

because of the conditions on causality and stability for (16). Likewise the transfer function for the transformed filter is

$$H_1(\hat{z}_1\hat{z}_2^{\beta/\alpha})=\sum_{m=0}^{+\infty}h(m,0)(\hat{z}_1\hat{z}_2^{\beta/\alpha})^m \tag{23}$$

and (21), (22) are still valid here; hence the stability is not affected by the transformation. Note that the new coordinate system is employed to define grid points in the spatial domain of the transformed filter (see Fig. 7).

Thus far we have considered the transformation of two-dimensional digital filters with one variable. In general there is no restriction to the type of transfer function to which the transformation of (17) is applicable. However, our attention will be limited to separable prototype filters throughout this paper so that the two-dimensional filtering operation can be realized as a series of one-dimensional filtering operations.

For a separable filter which is stable and causal such that

$$H(z_1,z_2)=H_1(z_1)H_2(z_2) \tag{24}$$

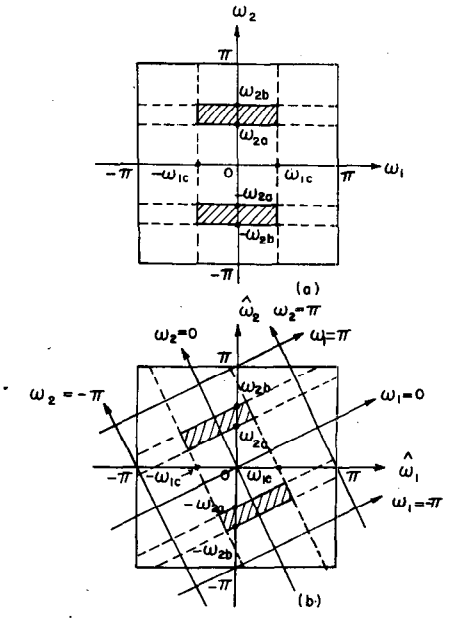

Fig. 3. Frequency response of bandpass filter of (24) and its rotated version.

consider the transformation

$$z_1=\hat{z}_1\hat{z}_2^{\beta/\alpha}$$
$$z_2=\hat{z}_1^{\beta/\alpha}\hat{z}_2^{-1} \tag{25}$$

where α and β are integers. The transformed frequency response may be obtained as

$$\omega_1 L_1=\hat{\omega}_1\hat{L}_1+\left(\frac{\beta}{\alpha}\right)\hat{\omega}_2\hat{L}_2$$
$$\omega_2 L_2=\left(\frac{\beta}{\alpha}\right)\hat{\omega}_1\hat{L}_1-\hat{\omega}_2\hat{L}_2 \tag{26}$$

where $L_1^2=\hat{L}_1^2+(\beta/\alpha\hat{L}_2)^2$, $L_2^2=(\beta/\alpha\hat{L}_1)^2+\hat{L}_2^2$ and the angle of rotation is the same as (19). This relation is illustrated in Fig. 3, where $H_1(z_1)$ is a low-pass filter and $H_2(z_2)$ is a bandpass filter. Note that there are 6 fixed points under the mapping of (26), and they are $(\pm\omega_{1c},0)$, $(0,\pm\omega_{2a})$ and $(0,\pm\omega_{2b})$. The ratio of linear contraction of the pass region incurred by the transformation is generally given by $\cos\theta$ ($\theta=\arctan(\beta/\alpha)$) as before.

In addition it may be observed that the rotation of the Nyquist frequencies yields the reduction of the effective frequency range. Hereafter, we will refer to the effective frequency range as the Nyquist region. In Fig. 4, four possible recursion directions are shown with their corresponding transformations. With these recursion directions the Nyquist region will contract as shown in Fig. 5(a). The minimum Nyquist region occurs when $\beta/\alpha=1$ in (25) as shown in Fig. 5(b).

Finally let us consider the range of α and β. When β/α is an integer, the transformation falls in the category of ordinary two-dimensional frequency transformations [9].

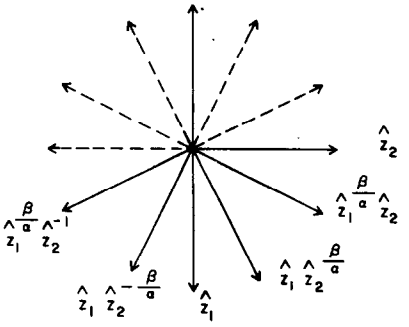

Fig. 4. Four possible recursion directions with corresponding transformations given α and β.

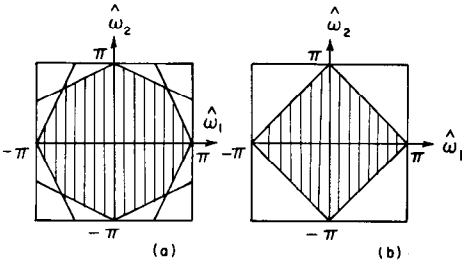

Fig. 5. Contracted Nyquist region ($\beta/\alpha=\frac{1}{2}$) and minimum Nyquist region ($\beta/\alpha=1$).

When $\beta/\alpha>1$, one may choose alternative transformations such as $\hat{z}_1^{\alpha/\beta}\hat{z}_2$ in which the sample interval is shorter than for (17). Therefore there is no loss of generality if we restrict α and β such that $\alpha \geqslant \beta$, α and β are integers.

IV. Implementation of the (z_1,z_2)-Plane Rotated Filters by Employing Interpolated Filter Systems

The previous section describes the rotation of separable filter frequency responses using the transformation of (17). However, this transformation is not readily applicable to standard rectangular arrays since the signal values for the transformed filter are not defined at the new grid points. If one uses a suitable interpolation function, that can reconstruct a continuous signal from a discrete signal, it is possible to generate an interpolated array where signal values are defined on the new grid points. Several interpolation functions are briefly discussed in Section II-C.

Consider the two-dimensional band-limited interpolation function of (9). For a grid point at $x=iL_x$ and $y=(k+\Delta_i)L_y$ where Δ_i denotes the decimal part of $(\beta/\alpha)i$ [see Fig. 6]

$$f_{\text{int}}(i,k+\Delta_i)=\sum_{m=-\infty}^{+\infty}\sum_{n=-\infty}^{+\infty} f(m,n)\,\text{sinc}\,(i-m)\cdot\text{sinc}\,(k+\Delta_i-n)$$

$$=\sum_{n=-\infty}^{+\infty} f(i,n)\,\text{sinc}\,(k+\Delta_i-n) \qquad (27)$$

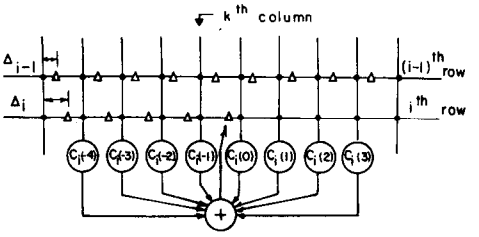

Fig. 6. Interpolation algorithm of (30) with $c_i(\hat{n})=\text{sinc}(\Delta_i-\hat{n})$ and $K=4$.

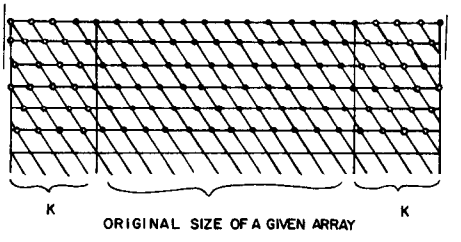

Fig. 7. Grid points of interpolated array with augmentation along z_1 direction ($\beta/\alpha=2/3$).

where i and k are integers and sinc $(i-m)=0$ except when $m=i$. Here, $f_{\text{int}}(i,k+\Delta_i)$ and $f(m,n)$ denote the interpolated and standard array values, respectively. Now there are two problems with the interpolation function of (27). First, the interpolated array is not bounded even for a bounded input array (k is not bounded in (27)). Second, the interpolation of (27) at each new grid point is computationally inefficient. One possible way of obtaining a meaningful interpolation function which approximates (27) would be to truncate the infinite series at $n=\pm K$.

Define the rectangular window and truncated interpolation function as follows:

$$\text{rect}\,(x)=\begin{cases}1, & -1/2\leqslant x\leqslant 1/2\\ 0, & \text{otherwise}\end{cases} \qquad (28)$$

$$\varphi_1(x)=\text{sinc}\,(x)\,\text{rect}\left(\frac{x}{2K}\right). \qquad (29)$$

With this new interpolation function $\varphi_1(x)$, one may approximate (27), i.e.,

$$f_{\text{int}}(i,k+\Delta_i)\approx\sum_{n=-\infty}^{+\infty} f(i,n)\varphi_1(k+\Delta_i-n)$$

$$=\sum_{\hat{n}=-K+1}^{K}\text{sinc}\,(\Delta_i-\hat{n})f(i,k+\hat{n})$$

$$=\hat{f}\,(i,k+\Delta_i) \qquad (30)$$

where $\hat{n}=n-k$ and $\hat{f}(i,k+\Delta_i)$ represents an interpolated array which is augmented by length $2K$ along the interpolating direction. Furthermore, $\hat{f}(i,k+\Delta_i)$ is bounded in the same manner as the original array. The interpolation algorithm is illustrated in Fig. 6 and the grid points of an interpolated array are shown in Fig. 7. Note that the

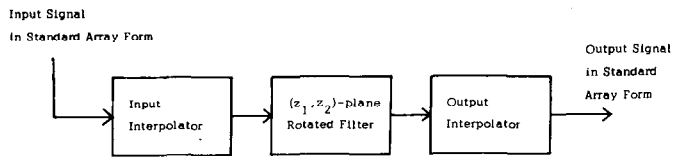

Fig. 8. Interpolated filter system.

interpolation occurs row by row. With the interpolated array shown in Fig. 7, one can perform recursive filtering in the new direction. The output array will have the same grid points as shown in Fig. 7. To convert the output signal array to standard array form, one needs array interpolation once more. The augmented portion of the array is necessary only to produce the output in standard array form. Thus the domain of the final output array is the same as that of the input array. Consequently two interpolation operations are necessary to realize the transformation of (17), an input interpolation and an output one.

There are several facts worth noting concerning the interpolation scheme of (30).

1) It may be regarded as a moving average estimator where the set of coefficients is determined by the interpolation function $\varphi_1(x)$ and the interpolating distance Δ_i which is a function of row index $i(0 \leqslant \Delta_i < 1$ for a unit sample distance).

2) The interpolation operation is not performed uniformly on the given data array. At the rows where given and new grid points coincide, the interpolation operation is no longer necessary ($\Delta_i = 0$).

3) It does not pose any stability problem because it is a FIR (finite impulse response)-type estimator.

V. Frequency Responses of the Interpolated Filter Systems

An interpolated filter system that consists of input/output interpolators and a (z_1,z_2)-plane rotated filter is shown in Fig. 8. The necessity of input/output interpolators at both ends of the (z_1,z_2)-plane rotated filter is obvious in view of the discussion above. Therefore the overall frequency response of the interpolated filter system is determined by the input/output interpolators as well as by the (z_1,z_2)-plane rotated filter. The frequency response of the interpolation function can easily be obtained by Fourier transforming the interpolation function $\varphi(x)$. When the interpolation function is $\varphi_1(x)$ as in (29)

$$\begin{aligned} F\{\varphi_1(x)\} &= F\left\{\text{sinc}\,(x)\,\text{rect}\left(\frac{x}{2K}\right)\right\} \\ &= F\{\text{sinc}\,(x)\} * F\left\{\text{rect}\left(\frac{x}{2K}\right)\right\} \\ &= \text{rect}\left(\frac{\omega_x}{2\pi}\right) * \left[2K \cdot \text{sinc}\left(\frac{2K\omega_x}{2\pi}\right)\right] \end{aligned} \tag{31}$$

where "*" denotes convolution.

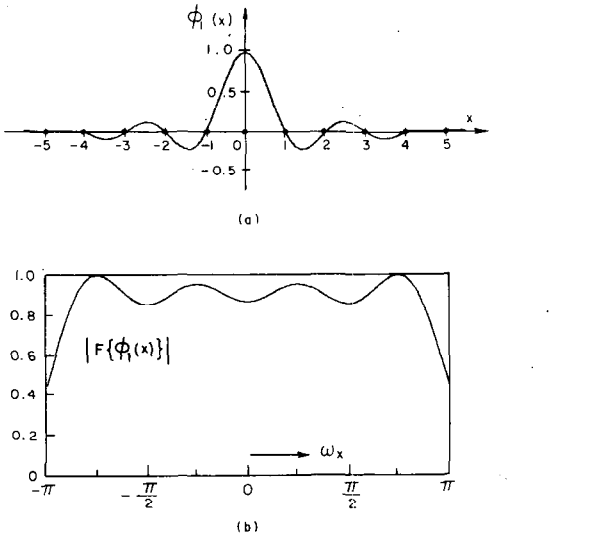

Fig. 9. Truncated interpolated function $\varphi_1(x)$ of (29) with $K=4$ and its frequency characteristic.

The interpolation function $\varphi_1(x)$ and its Fourier transform are shown in Fig. 9. In Fig. 9(b), one may observe the overshooting caused by the rectangular window. As already known in the theory of finite impulse response (FIR) filters, the use of generalized windows such as the Hamming, Hanning or Kaiser windows will improve the frequency characteristics of the interpolation function. For example, we may use the generalized Hamming window defined as

$$q_K(x) = \left[r + (1-r)\cos\left(\frac{2\pi x}{2K}\right)\right] \text{rect}\left(\frac{x}{2K}\right), \qquad 0 \leqslant r \leqslant 1. \tag{32}$$

The resulting interpolation function is

$$\varphi_2(x) = \text{sinc}\,(x) q_K(s). \tag{33}$$

$\varphi_2(x)$ with $r=0.7$ and $K=4$ and its frequency characteristic are shown in Fig. 10. Note that the frequency characteristic of $\varphi_2(x)$ is fairly flat except in the vicinity of the Nyquist frequency. Since there are two interpolators for input/output and their characteristics are identical, the overall frequency characteristic for both input/output interpolators may be denoted by $[F\{\varphi(x)\}]^2$. As long as one is concerned with the frequency transformation of (17), interpolation occurs along one direction only, either the z_1 or z_2 direction. Thus the frequency characteristic along the other direction is not affected. Although the Fourier transform of an interpolation function may represent the frequency characteristic of input/output interpolators, it is not exactly the same as the actual characteristic since interpolations are not carried out uniformly. For instance, referring to Fig. 7, the first and fourth rows of the array are not interpolated while the second and third rows are. Therefore, it may hold in an actual case that the frequency characteristic of the input/output interpolators is better than that given by the Fourier transform of the

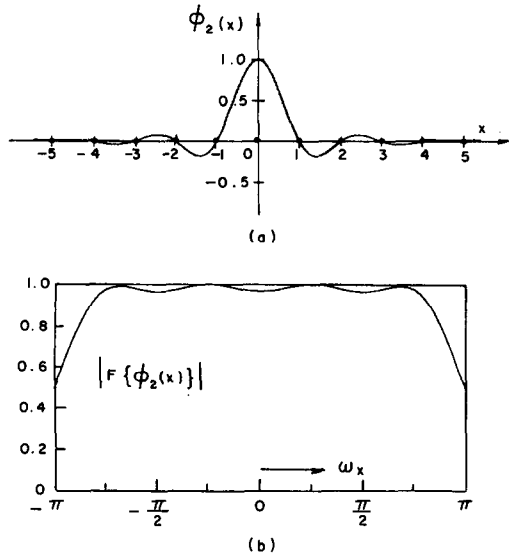

Fig. 10. Interpolation function $\varphi_2(x)$ of (33) using Hamming window ($r=0.7$ and $K=4$) and its frequency characteristic.

interpolation function. An alternate way of finding the frequency characteristic of the interpolated filter system is to apply the discrete Fourier transform (DFT) to the impulse response.

Example 1: Given the one-dimensional 6th-order low-pass filter

$$H_1(z)=(10^{-2})(0.1052+0.6340z+1.5775z^2+2.1033z^3+1.5775z^4+0.6340z^5+0.1052z^6)/(1-2.9785z+4.1361z^2-3.2598z^3+1.5173z^4-0.3911z^5-0.0434z^6)$$

one may find the frequency responses of the interpolated filter system for $H_1(\hat{z}_1\hat{z}_2^{1/2})$ and Shanks' rotated filter, and compare the two using the interpolation function $\varphi_2(x)$ of (33) with $r=0.7$ and $K=4$ (8 terms).

The overall frequency response of the interpolated filter system is obtained from the DFT of its impulse response. To include the effect of the input interpolator, the first row is interpolated where the impulse is applied. The amplitude response of the one-dimensional prototype filter in two dimensions is shown in Fig. 11(a). The amplitude responses of Shanks' rotated filter and the interpolated filter system are shown in Fig. 11(b) and (c), respectively. In Fig. 11, the amplitude responses are displayed in 16 grey levels.

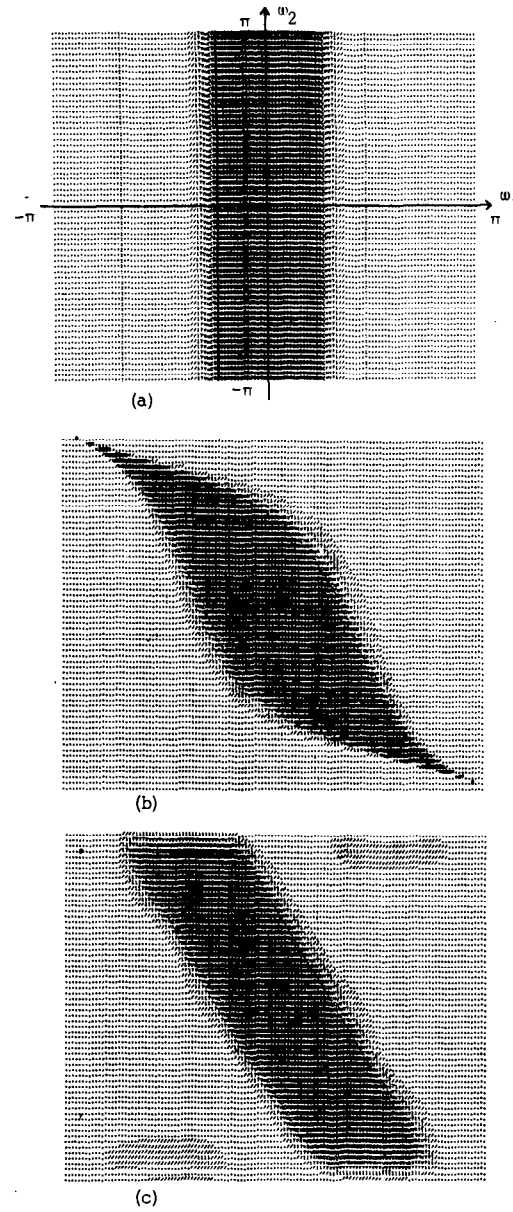

Fig. 11. Amplitude responses of Example 1; (a) prototype filter, (b) Shanks' rotated filter, (c) interpolated filter systems.

VI. Design Techniques Using Interpolated Filter Systems

In this section, design techniques of two-dimensional recursive filters using interpolated filter systems are illustrated through three examples:

1) a circularly symmetric low-pass filter,
2) a nonseparable bandpass filter,
3) a ring-shaped bandpass filter.

Two inherent problems in employing interpolated filter systems are the high-frequency attenuation in the vicinity of the Nyquist frequencies, caused by windowing of the interpolation function, and the contraction of the Nyquist region resulting from the frequency response rotation [see Fig. 5]. Because of the first problem, high-pass interpolated filter systems should be used with *a priori* spectral considerations of the input signal. Due to the second problem, the presence of undesired pass regions beyond the contracted Nyquist region is possible in interpolated filter systems. However, the two problems above are not serious drawbacks in practical applications.

In the following examples, we assume that the input signals are given as finite area arrays so that noncausal filters can be realized through the array reorientations listed in Section II-B. Also, we employ the zero-phase

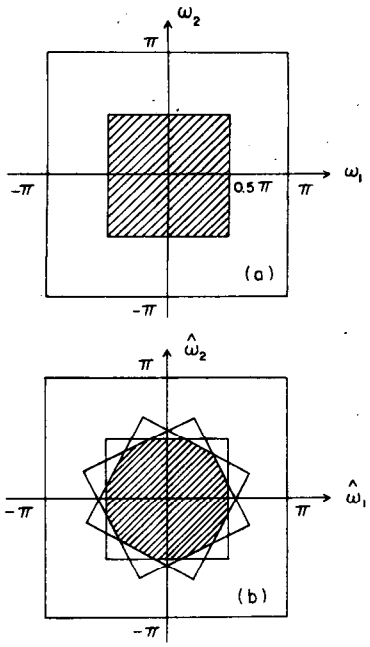

Fig. 12. Approximation of circularly symmetric low-pass filter; (a) prototype filter, (b) its rotated filters and cascading of these three for Example 2.

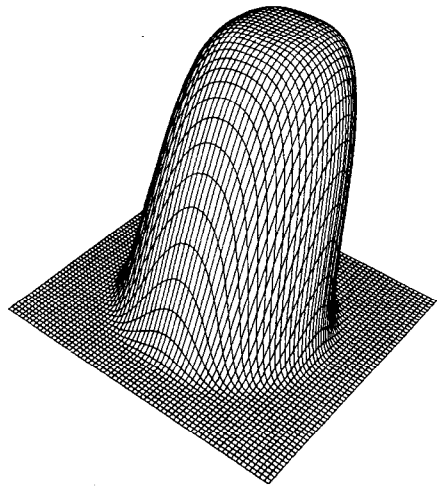

Fig. 13. Actual amplitude response of Fig. 12(b) for Example 2.

implementations for the given amplitude specifications. As one-dimensional filters, bilinear transformed Butterworth filters are used. For an interpolation function, $\varphi_2(x)$ of (33) is applied with $r=0.5$ and $K=4$. Input/output interpolators are denoted by "[" and "]", respectively, in the transfer function expressions of the following examples.

Example 2: Design a circularly symmetric low-pass filter with the following specifications:

$$0.8 \leqslant |H(e^{-j\hat{\omega}_1}, e^{-j\hat{\omega}_2})| \leqslant 1.0, \qquad \rho \leqslant 0.5\pi$$

$$0 \leqslant |H(e^{-j\hat{\omega}_1}, e^{-j\hat{\omega}_2})| \leqslant 0.1, \qquad \rho \geqslant 0.65\pi$$

where $j=\sqrt{-1}$ and $\rho^2=\hat{\omega}_1^2+\hat{\omega}_2^2$.

The pass region is approximated by cascading three

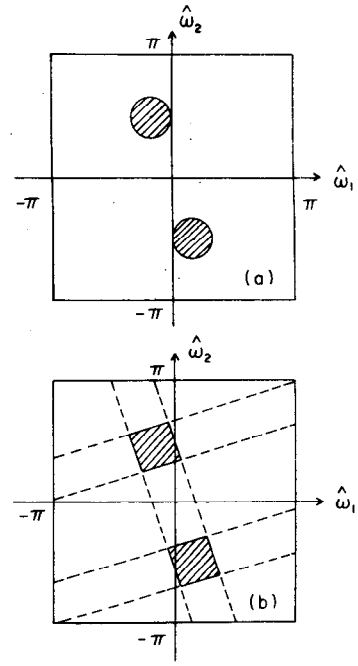

Fig. 14. (a) Specification and (b) approximation for Example 3.

basic filter sections, a prototype filter and two rotated filters, as shown in Fig. 12. The basic angle of rotation used is 26.6° ($\theta=\arctan(1/2)$). Because of the bandwidth contraction in the frequency transformation, two one-dimensional filters, $H_1(z)$ and $H_2(z)$, with different cutoff frequencies are used to derive three basic filter sections. The overall amplitude response is shown in Fig. 13 and the transfer function is

$$H(\hat{z}_1,\hat{z}_2)=HX(\hat{z}_1,\hat{z}_2)HY(\hat{z}_1,\hat{z}_2)HZ(\hat{z}_1,\hat{z}_2)$$

where

$$HX(\hat{z}_1,\hat{z}_2)=HL_1(\hat{z}_1)HL_1(\hat{z}_1^{-1})HL_1(\hat{z}_2)HL_1(\hat{z}_2^{-1})$$

$$HY(\hat{z}_1,\hat{z}_2)=\left[HL_2(\hat{z}_1\hat{z}_2^{1/2})HL_2(\hat{z}_1^{-1}\hat{z}_2^{-1/2})\right]\cdot\left[HL_2(\hat{z}_1^{-1/2}\hat{z}_2)HL_2(\hat{z}_1^{1/2}\hat{z}_2^{-1})\right]$$

$$HZ(\hat{z}_1,\hat{z}_2)=\left[HL_2(\hat{z}_1\hat{z}_2^{-1/2})HL_2(\hat{z}_1^{-1}\hat{z}_2^{1/2})\right]\cdot\left[HL_2(\hat{z}_1^{1/2}\hat{z}_2)HL_2(\hat{z}_1^{-1/2}\hat{z}_2^{-1})\right]$$

$$HL_1(z)=(0.39662+0.79325z+0.39662z^2)/(1+0.38816z+0.19833z^2)$$

$$HL_2(z)=(0.47658+0.95317z+0.47658z^2)/(1+0.65732z+0.24901z^2).$$

Example 3: Design a nonseparable bandpass filter with the following characteristic [see Fig. 14(a)]:

$$0.707 \leqslant |H(e^{-j\hat{\omega}_1}, e^{-j\hat{\omega}_2})| \leqslant 1, \qquad \rho \leqslant \frac{\pi}{6}$$

$$0 \leqslant |H(e^{-j\hat{\omega}_1}, e^{-j\hat{\omega}_2})| \leqslant 0.2, \qquad \rho \geqslant \frac{\pi}{3}$$

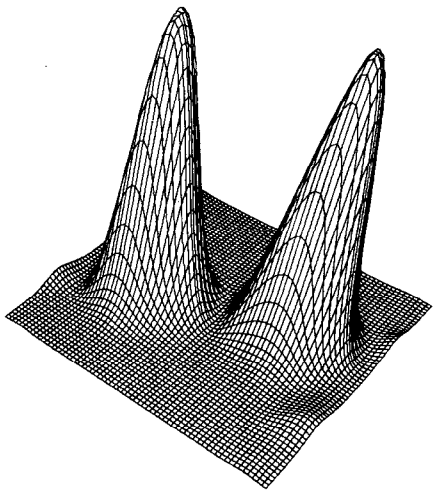

Fig. 15. Actual amplitude response of Fig. 14(b) for Example 3.

where

$$\rho^2=\left(\hat{\omega}_1+\frac{\pi}{6}\right)^2+\left(\hat{\omega}_2-\frac{\pi}{2}\right)^2$$

or

$$\rho^2=\left(\hat{\omega}_1-\frac{\pi}{6}\right)^2+\left(\hat{\omega}_2+\frac{\pi}{2}\right)^2.$$

The pass region is approximated by rotating a separable filter as shown in Fig. 14(b). The basic angle of rotation used is 18.4° ($\theta=\arctan(1/3)$). The amplitude response of the actual filter is shown in Fig. 15 and the transfer function is given as follows:

$$H(\hat{z}_1,\hat{z}_2)=\left[HL\left(\hat{z}_1\hat{z}_2^{1/3}\right)HL\left(\hat{z}_1^{-1}\hat{z}_2^{-1/3}\right)\right]\cdot\left[HB\left(\hat{z}_1^{-1/3}\hat{z}_2\right)HB\left(\hat{z}_1^{1/3}\hat{z}_2^{-1}\right)\right]$$

where

$$HL(z)=(0.07672+0.15344z+0.07672z^2)/(1-1.07832z+0.38519z^2)$$

$$HB(z)=0.47260(1-z^2)/(1+0.08936z+0.05481z^2).$$

Example 4: Design a ring-shaped bandpass filter with the following specifications:

$$0.707\leqslant|H(e^{-j\hat{\omega}_1},e^{-j\hat{\omega}_2})|\leqslant 1,\qquad 0.4\pi\leqslant\rho\leqslant 0.6\pi$$

$$0\leqslant|H(e^{-j\hat{\omega}_1},e^{-j\hat{\omega}_2})|\leqslant 0.05,\qquad \rho\leqslant 0.3\pi \text{ or } \rho\geqslant 0.75\pi$$

where

$$\rho^2=\hat{\omega}_1^2+\hat{\omega}_2^2.$$

As a first step, a prototype filter with the frequency response shown in Fig. 16(a) is realized by paralleling two separable filters. Two different realizations are available in doing this: one of them is partitioning the pass region into four strips as shown in Fig. 16(a), while the other is

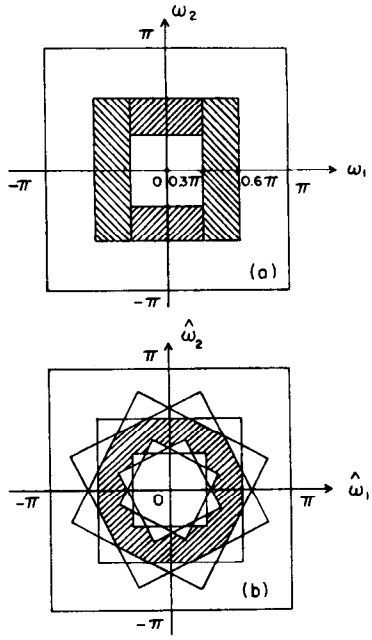

Fig. 16. Approximation of ring-shaped bandpass filter; (a) prototype filter, (b) its rotated filters and cascading of these three for Example 4.

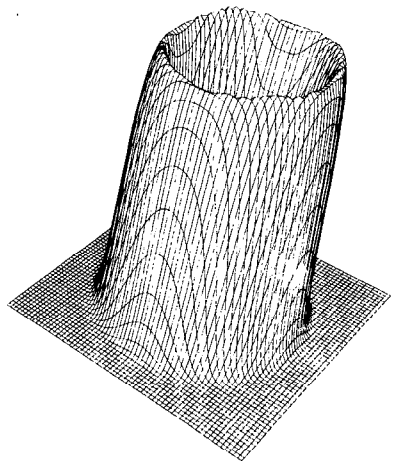

Fig. 17. Actual amplitude response of Fig. 16(b) for Example 4.

subtracting the inner rectangular pass region from the outer one. The latter scheme, which is used in this example, becomes possible because of the zero-phase characteristic. Now the desired response may be approximated by cascading three basic filter sections, a prototype filter and its two rotated filters, as shown in Fig. 16(b). The basic angle of rotation used is 26.6° ($\theta=\arctan(1/2)$). The amplitude response is shown in Fig. 17 and the overall transfer function is

$$H(\hat{z}_1,\hat{z}_2)=HX(\hat{z}_1,\hat{z}_2)HY(\hat{z}_1,\hat{z}_2)HZ(\hat{z}_1,\hat{z}_2)$$

where

$$HX(\hat{z}_1,\hat{z}_2)=HL_3(\hat{z}_1)HL_3(\hat{z}_1^{-1})HL_3(\hat{z}_2)HL_3(\hat{z}_2^{-1})-HL_4(\hat{z}_1)HL_4(\hat{z}_1^{-1})HL_4(\hat{z}_2)HL_4(\hat{z}_2^{-1})$$

TABLE I

$H(z) = (a_0 + a_1 z + a_2 z^2 + a_3 z^3)/(1 + b_1 z + b_2 z^2 + b_3 z^3)$

	a_0	a_1	a_2	a_3	b_1	b_2	b_3
HL_3	0.46904	0.93809	0.46904	0	0.63289	0.24329	0
HL_4	0.04562	0.13658	0.13658	0.04562	-1.22105	0.73445	-0.14846
HL_5	0.56781	1.13562	0.56781	0	0.93919	0.33206	0
HL_6	0.05975	0.17925	0.17925	0.05975	-1.01921	0.61133	-0.11416

$$HY(\hat{z}_1,\hat{z}_2) = \left[HL_5(\hat{z}_1\hat{z}_2^{1/2})HL_5(\hat{z}_1^{-1}\hat{z}_2^{-1/2})\right] \cdot \left[HL_5(\hat{z}_1^{-1/2}\hat{z}_2)HL_5(\hat{z}_1^{1/2}\hat{z}_2^{-1})\right] - \left[HL_6(\hat{z}_1\hat{z}_2^{1/2})HL_6(\hat{z}_1^{-1}\hat{z}_2^{-1/2})\right] \cdot \left[HL_6(\hat{z}_1^{-1/2}\hat{z}_2)HL_6(\hat{z}_1^{1/2}\hat{z}_2^{-1})\right]$$

$$HZ(\hat{z}_1,\hat{z}_2) = HY(\hat{z}_1,\hat{z}_2^{-1}).$$

The one-dimensional filters HL_3, HL_4, HL_5, and HL_6 are listed in the Table I.

As seen in the examples, an interpolated filter system may be used to synthesize a two-dimensional recursive filter with a desired frequency response. Any convex low-pass shape in the frequency domain can be approximated by a convex polygon, which may be realized by cascading (z_1,z_2)-plane rotated filters. As a general approach to approximating a given frequency response, partitioning a complicated pass region into several elementary contiguous pass regions might be useful. An elementary pass region is one that can be realized by cascading (z_1,z_2)-plane rotated filters. To get an overall frequency response, one can sum up elementary contiguous pass regions. This is equivalent to paralleling elementary filters. Unlike the case for one-dimensional filters there is in general no cascade implementation which is equivalent to a parallel implementation in the case of two- or multi-dimensional filters. This is due to the lack of a factorization theorem in polynomials of two or more variables. If one tries to make use of the partitioning technique in realizing a nonzero phase two-dimensional filter, one may not avoid borderline matching problems between elementary contiguous pass regions.

There are a few more comments worth noting in conjunction with Example 1. J. Costa and A. Venetsanopoulos have suggested a design technique for a circularly symmetric low-pass filter using Shanks' rotated filters [10]. In their work the desired frequency response is synthesized by cascading two elliptically shaped filters with data rotations of 90°. An elliptically shaped filter designed as a basic filter section is obtained by cascading three 2nd-order Butterworth filters rotated by 285°, 315°, and 345°.

In our Example 2, a basic filter section is obtained by cascading two (z_1,z_2)-plane rotated filters with interpolators. Each rotated filter consists of one-dimensional filters whereas Shanks' rotated filter consists of two-dimensional filters. For the case of Example 2, it is hard to say which technique is better. Each design technique involves many problems such as the degree of approximation, the complexity of the implementation and the performance of the filter. However, one may observe that an interpolated filter system provides a designer with more flexibility than Shanks' rotated filters when one approximates frequency responses such as those of Examples 3 and 4.

VII. Conclusion

The problem of rotating a separable filter response through an interpolated filter system has been studied. Since a separable filter basically consists of one-dimensional filters, for which software and hardware structures are extremely simple over two- or multi-dimensional filters, our attention has been limited to the rotation of a separable filter response and its applications. A primary advantage of employing separable filters in interpolated filter systems is that one may perform two- or multi-dimensional manipulations by means of a series of one-dimensional manipulations. With this scheme the same interpolated filter system may be used iteratively, together with proper array reorientations, resulting in an appreciable saving in hardware.

Although most of the input signals are assumed to be finite area arrays throughout the paper, this condition may be weakened depending on the recursion direction and the input data structure. We have discussed a general approach to designing two-dimensional recursive filters in the frequency domain employing interpolated filter systems. Further work is needed to generalize the technique.

References

[1] J. L. Shanks, S. Treitel, J. H. Justice, "Stability and synthesis of two-dimensional recursive filters," *IEEE Trans. on Audio and Electroac.*, vol. AU-20, pp. 115–128, June 1972.

[2] M. T. Manry and J. K. Aggarwal, "Picture processing using one-dimensional implementations of discrete planar filters," *IEEE Trans. on Acoustics, Speech, and Signal Proc.*, vol. ASSP-22, pp. 164–173, June 1974.

[3] R. M. Mersereau and D. E. Dudgeon, "The representation of two-dimensional sequences as one-dimensional sequences," *IEEE Trans. on Acoustics, Speech and Signal Proc.*, vol. ASSP-22, pp. 320–325, Oct. 1974.

[4] S. Treitel and J. L. Shanks, "The design of multistage separable planar filters," *IEEE Trans. on Geoscience Electronics*, vol. GE-9, pp. 10–27, Jan. 1971.

[5] A. V. Oppenheim and R. W. Schafer, *Digital Signal Processing* Englewood Cliffs, NJ: Prentice Hall, 1975.
[6] L. R. Rabinar and B. Gold, *Theory and Application of Digital Signal Processing*. Englewood Cliffs, NJ: Prentice Hall, 1975.
[7] A. Papoulis, *The Fourier Integral and its Applications*. New York: McGraw-Hill, 1962.
[8] J. W. Goodman, *Introduction to Fourier Optics*. New York: McGraw-Hill, 1968.
[9] N. A. Pendergrass, S. K. Mitra, and E. I. Jury, "Spectral transformations for two-dimensional digital filters," in *IEEE Proc., Symposium on Circuits and Systems*, Apr. 1975.
[10] J. M. Costa and A. N. Venetsanopoulos, "Design of circularly symmetric two-dimensional recursive filters," *IEEE Trans. on Acoustics, Speech, and Signal Proc.*, vol. ASSP-22, Dec. 1974.

Hyokang Chang was born in Seoul, Korea, on July 22, 1947. He received the B.S. degree from Seoul National University, Seoul, Korea, in 1970. He was admitted to the University of Texas, Austin, in January 1974, as a graduate student in the Department of Electrical Engineering and received the M.S. degree in 1975. He is presently a Research Assistant at the University of Texas at Austin, while continuing his graduate studies.

His main research interest is two-dimensional signal processing.

J. K. Aggarwal (S'62–M'65–SM'74–F'76) was born in Amritsar, India, on November 19, 1936. He was educated in India, England, and the U.S.A. He received the B.S. in mathematics and physics from the University of Bombay (1956), Bombay, India; the B. Eng. degree from the University of Liverpool, Liverpool, England (1960), and the M.S. and Ph.D. degrees at the University of Illinois, Urbana, in 1961 and 1964, respectively.

He joined the University of Texas, Austin, in 1964 as an Assistant Professor and has since held positions as Associate professor (1968) and Professor (1972). Currently, Dr. Aggarwal is a Professor of Electrical Engineering and of Computer Science at the University of Texas at Austin. Further, he was a Visiting Assistant Professor to Brown University, Providence, RI (1968), and a Visiting Associate Professor at the University of California, Berkeley, during 1969–1970. He has published numerous technical papers and a text book, *Notes on Nonlinear Systems*, published by Van Nostrand Reinhold, in 1972, in the series Notes on System Sciences. His current research interests are digital filters, computational methods, image processing and computer pattern recognition.

Dr. Aggarwal was an ADCOM member of the Circuits and Systems Society, 1972–1975; Chairman of the Technical Committee on Signal Processing, 1974–1975; the Associate Editor of the IEEE TRANSACTIONS ON CIRCUITS AND SYSTEMS, 1973–1975; and Co-Editor of its Special Issue on Digital Filtering and Image Processing, March 1975, and the Editor of the Circuits and Systems Society Newsletter, 1971–1972. He is also a member of Eta Kappa Nu.

Control of Limit Cycles in Recursive Digital Filters by Randomized Quantization

R. BRUCE KIEBURTZ, SENIOR MEMBER, IEEE, VICTOR B. LAWRENCE, AND KENT V. MINA

Abstract—**The different types of limit cycles which can occur in single second-order sections respond differently to efforts to reduce them. Length 1 (dc) limit cycles play an important complicating role, especially in cascaded filters. We describe a simple method, involving random requantization of multiplier outputs, which can reduce or eliminate limit cycles in digital filters. We compare limit cycle and roundoff noise in three typical low-pass filters with and without the method.**

I. INTRODUCTION

THE PERFORMANCE of fixed point recursive digital filters is degraded by the requantization of products at the output of multipliers. The resulting errors are observed as roundoff noise during signal processing or as limit cycle oscillations during idle channel conditions. The usual procedure for ensuring that either or both of these effects are tolerable is to increase the internal wordlength of the filter. For example a high performance low-pass filter used 15-bit input data and 21-bit internal data [1]. In principle either the roundoff noise or the limit cycle behavior may dominate in setting the required internal data wordlength. This paper discusses techniques for suppressing limit cycles by randomly switching the quantization between truncating and rounding [2]. This allows the internal data wordlength, hence the required memory, to be determined by signal to roundoff noise considerations.

The implementation for which randomized quantization is analyzed is a cascade of second-order sections. The

Manuscript received July 29, 1976; revised February 5, 1977.
The authors are with Bell Telephone Laboratories, Holmdel, NJ 07733.